

## Processing and characterisation of plasma sprayed zirconia–alumina–mullite composite coating on a mild-steel substrate

S. DAS

*Department of Metallurgical and Materials Engineering, Indian Institute of Technology, Kharagpur–721 302, India*

S. GHOSH

*Department of Mechanical Engineering, Indian Institute of Technology, Kharagpur–721 302, India*

A. PANDIT, T. K. BANDYOPADHYAY

*Department of Metallurgical and Materials Engineering, Indian Institute of Technology, Kharagpur–721 302, India*

A. B. CHATTOPADHYAY

*Department of Mechanical Engineering, Indian Institute of Technology, Kharagpur–721 302, India*

K. DAS

*Department of Metallurgical and Materials Engineering, Indian Institute of Technology, Kharagpur–721 302, India*

Out of many surface modification techniques, plasma spraying stands out as one of the most versatile and technologically sophisticated thermal spraying technique. One limitation of the process is the high price of “plasma sprayable”, dedicated consumables. However, in a recent study, ceramic powders like zircon and alumina of commercial variety have been successfully used as plasma sprayable consumables [1, 2]. Plasma sprayed, ceramic-coated components are used in a number of engineering applications, especially where wear resistance and resistance to high temperature are important [3]. Alumina and zirconia are examples of plasma spraying consumables, which are used frequently in such applications. Zirconia–mullite ceramic composite is a potential candidate for high temperature and wear applications [4]. Mullite possesses interesting physical properties, such as low thermal expansion, creep resistance, low thermal conductivity, and high chemical stability. Zirconia, on the other hand, improves the toughness of the composite [5]. Zirconia–mullite composite is often produced by CVD, sol–gel method and reaction sintering of zircon and alumina, where at a high temperature silica is released from zircon and unites with alumina to form mullite [6–8]. However, development of such composite coating through reactive plasma spraying of zircon and alumina is not a common practice.

In this paper, an attempt has been made to develop zirconia–alumina–mullite composite coating through reactive plasma spraying of zircon and alumina. For this purpose, commercial grade alumina and zircon sand were used. The coating thus developed was tested for its performances in wear and cyclic thermal loading. Its wear performance is compared with plasma sprayed zircon sand coating and another coating made from imported, plasma grade alumina powder.

As-received zircon sand was ball milled in a planetary ball mill and subsequently sieved to a size range of 45–100  $\mu\text{m}$ . The alumina–zircon weight percentage is decided as per the ternary diagram of alumina–zirconia–silica [9]. It is observed that to obtain mullite the  $\text{Al}_2\text{O}_3/\text{SiO}_2$  ratio of the plasma consumable should be 3:2 (mol%) as per the stoichiometry. Since, in the plasma arc 1 mole of  $\text{ZrSiO}_4$  is dissociated into 1 mole of  $\text{ZrO}_2$  and 1 mole of  $\text{SiO}_2$ , the appropriate  $\text{Al}_2\text{O}_3/\text{ZrSiO}_4$  ratio for complete formation of mullite is 3:2 (in mol%) or 55% of  $\text{Al}_2\text{O}_3$  and 45% of  $\text{ZrSiO}_4$  (in wt%). The blending was carried out in a planetary ball mill in dry condition for 25 min. The alumina and zircon used in this experiment are of commercial variety (Indian origin) and as such do not belong to the so called “plasma sprayable” category.

The blend thus obtained was plasma sprayed onto mild steel test coupons of dimensions  $160 \times 13 \times 5$  mm using a plasma spraying equipment of capacity of 40 kw. Before spraying, the mild steel substrates were shot blasted with alumina grits (grit size 60) and then cleaned using trichloroethylene and isopropyl alcohol in an ultrasonic cleaner. The cleaned specimens were plasma sprayed with Ni–5 wt% Al and high carbon iron bond coats and subsequently the top coats were sprayed on. After spraying, test coupons of dimensions  $10 \times 13 \times 5$  mm were cut off from the large samples for characterisation.

The top coat and the powders were examined for the identification of crystalline phases present in them using an X-ray diffractometer equipped with a cobalt target. For the scanning electron microscopy of the coatings, in cross section as well as top surface, these specimens were polished using diamond pastes. For thermal cycling, the specimens were soaked in a muffle furnace at 1100 °C for 1 hr followed by 10 min of

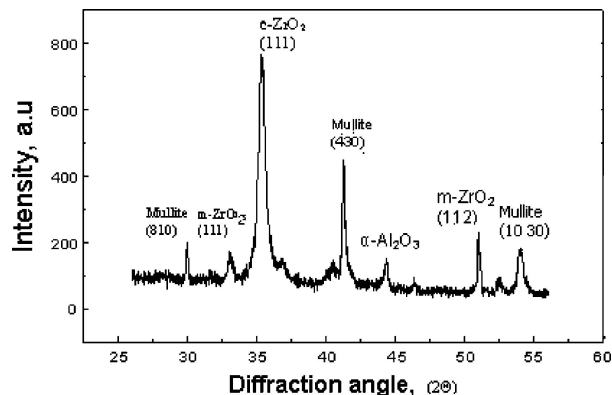


Figure 1 XRD pattern of the as-sprayed zircon–alumina coating.

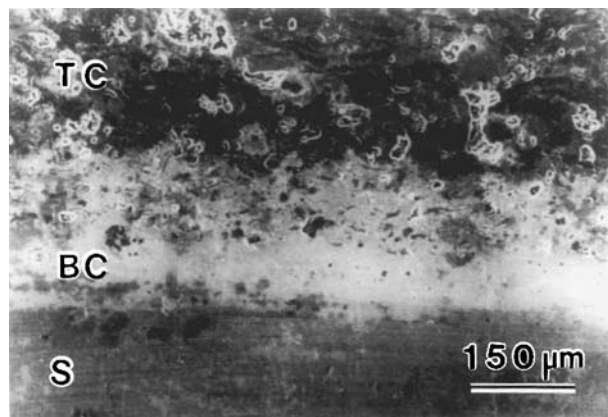


Figure 2 SEM micrograph (secondary electron image) of the zircon–alumina coating in cross section.

cooling in air. Meanwhile, a thorough visual scrutiny of the specimens was undertaken to find out the extent of damage it had undergone within the substrates, the interface between the top coat and bond coat, and within the top coat itself. Such thermal cycle was repeated a number of times. The tribological test was conducted in a pin-on-disc type wear testing set up with a normal load of 12.66 N and a linear sliding speed of 1.29 m/s. SiC abrasive paper of grit size 320 served as the abrading surface. Wear was measured by the change in weight of the specimen.

X-ray diffraction pattern of the as-coated zircon and alumina is shown in the Fig. 1. It consists of peaks from  $\alpha$ -alumina, monoclinic zirconia, cubic zirconia, and mullite. In the high temperature plasma environment zircon dissociates to form zirconia and silica. The high temperature cubic zirconia phase is retained owing to the rapid cooling associated with the plasma spraying process. Mullite peaks are also obtained because at around 1500 °C alumina combines with silica to form mullite. However, a complete conversion of entire amount of alumina to form mullite has not taken place. Presumably, a very short time available within the plasma jet is not adequate for the reaction to be completed. Silica peak is not observed owing to the fact that it remains in the amorphous state caused by a rapid solidification.

The scanning electron micrograph of the cross section of zircon–alumina coating (Fig. 2) reveals that the substrate/bond coat and the bond coat/top coat inter-

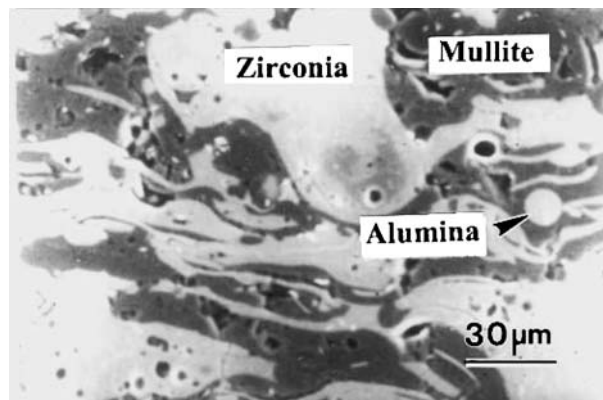


Figure 3 SEM micrograph (secondary electron image) of the polished top surface of the zircon–alumina coating.

faces are continuous and free from cracks. The coating appears to be very much adherent to the bond coat and quite dense. The SEM micrograph of the polished top surface of zircon–alumina coating (Fig. 3) shows a uniformly distributed multi phase mixture of alumina, mullite, and zirconia. Neither any major discontinuity nor any defect is found in the interphase boundary region or elsewhere on the polished top coat.

The performance of the coating under thermal cycling condition is mainly governed by the stresses developed at the coating/substrate interface owing to a difference in thermal expansion coefficients. This difference results in a shear stress at the interface, and it is responsible for the spallation of the coating. In addition, a thermally grown oxide layer (TGO) forms at the top coat/bond coat interface. It gradually grows with time and ultimately separates the coating from the substrate [10]. An iron bond coat is more vulnerable to oxidation as compared to its Ni–5 wt% Al counterpart. Under thermal cycling, the coating failure usually occurs through the formation of parallel cracks within the oxide layer near the topcoat/bond coat interface.

Table 1 shows the responses of the coatings to a cyclic thermal loading and it is also known as thermal fatigue behaviour. The material coated with zirconia–alumina–mullite top coat and Ni–5wt% Al bond coat offers better thermal fatigue resistance than the one coated with a high carbon iron bond coat. This is because of the diffusion of carbon and iron atoms between the high carbon iron bond coat and the steel substrate. This diffusion renders the bond coat somewhat ineffective. However, the main problem in this particular experiment is the oxidation of the mild steel substrate. In both cases, the tests are discontinued owing to an excessive substrate oxidation and not owing to a failure in either the top coat/bond coat or the bond coat/substrate interface. No significant cracking of the coatings is observed until the final cycles. This high thermal shock resistance of the top coats may be attributed to the presence of mullite, which increases fracture toughness. However, the point to be noted here is that the coatings are subjected to a very harsh testing condition, which is generally not experienced during applications.

The zirconia–alumina–mullite top coat shows a reasonably low wear (Fig. 4). The performance of the zirconia–alumina–mullite coating is compared with an

TABLE 1 Thermal fatigue behavior of the coatings under study

Top coat	Bond coat	No. of cycles conducted	Observations
Zircon–alumina	Ni–5% Al	24	Noticeable substrate oxidation occurs after few cycles. Thereafter, the deterioration of the substrate is quick owing to a rapid oxidation of the mild steel substrate. The coating and the bond coat are intact with no change in surface properties until around 15 cycles. Thereafter, the coating comes off along with the oxidized substrate along a surface away from the interface and well within the substrate. The top coat/bond coat interface remains intact. Finally, the top coat cracks after 24 cycles
Zircon–alumina	High carbon iron	15	The substrate oxidation occurs after initial few cycles and the oxidised layer grows rapidly. The coating starts peeling off after nine cycles, but again the plane of separation lies well within the substrate and away from either of the interfaces. The test was discontinued owing to a severe substrate oxidation

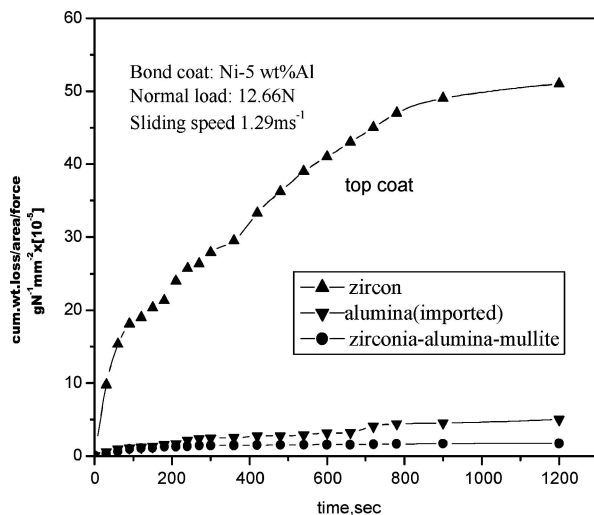


Figure 4 Cumulative weight loss in wears of as-sprayed zircon, zirconia–alumina–mullite and alumina (imported) coatings.

alumina coating deposited from a plasma-grade, imported consumable and a zircon sand coating. The wear performance of the zirconia–alumina–mullite composite coating is found to be better than the rest presumably owing to the presence of mullite. The presence of mullite delays the extent of wear by preventing crack propagation [11]. The reason for the increase in wear resistance may also be attributed to a higher fracture toughness of the composite coating. It is observed that a high fracture toughness increases wear resistance [12].

Plasma spraying of a mixture of zircon and alumina has been carried out on a mild steel substrate. The coating appears to be sound and continuous along the interfaces and in the bulk as well. During spraying, zircon sand dissociates into zirconia and silica and a fraction of this silica in turn combines with a fraction of alu-

mina to form the mullite phase. The presence of the mullite phase enhances the thermal fatigue characteristics of the coating. The failure of the coatings during cyclic thermal loading occurs mainly owing to the oxidation of the mild steel substrate. As a bond coat, the Ni–5 wt% Al is more effective than high carbon iron presumably for its enhanced capability to resist oxidation. The presence of mullite improves greatly on the wear performance of the composite coating.

## References

1. S. DAS, P. P. BANDYOPADHYAY, T. K. BANDYOPADHYAY, S. GHOSH and A. B. CHATTOPADHYAY, *Metall. Mater. Trans.* **34A** (2003) 1909.
2. S. DAS, P. P. BANDYOPADHYAY, S. GHOSH, T. K. BANDYOPADHYAY and A. B. CHATTOPADHYAY, *ibid.* **34A** (2003) 1919.
3. R. B. HEIMAN, in "Plasma Spray Coating, Principle and Application," (VCH, Weinheim, Germany, 1996) p. 343.
4. B. L. MITRA, M. K. BANERJEE, N. C. BISWAS and P. S. AGGARWAL, *Trans. Ind. Ceramic. Soc.* **44** (1985) 33.
5. J. S. MOYA and M. I. OSENDI, *J. Mater. Sci. Lett.* **2** (1983) 599.
6. M. L. AUGER, A. SENGUPTA and V. K. SARIN, *J. Amer. Cer. Soc.* **83** (2000) 2429.
7. F. KARA, S. TURAN, J. A. LITTLE and K. M. KNOWLESS, *ibid.* **83** (2000) 369.
8. R. TORRECILLAS, J. S. MOYA, S. D. AZA, H. GROS and G. FANTOZZI, *Acta. Metall. Mater.* **41** (1993) 1647.
9. E. M. LEVIN, C. R. ROBBINS and H. F. MCMURDIE, *Phase Diagrams for Ceramists*, 2nd edn., (The American Ceramic Society, OH, USA, 1969) p. 262.
10. H. M. CHOI, B. S. KANG, W. M. CHOI, D. G. CHOI, S. K. CHOI, J. C. KIM, Y. K. PARK and G. M. KIM, *J. Mater. Sci.* **33** (1998) 5895.
11. E. MEDVEDOVSKI, *Wear* **249** (2001) 821.
12. B. R. MARPLE and D. J. GREEN, *J. Amer. Ceramic. Soc.* **74** (1991) 2453.

Received 3 February  
and accepted 15 April 2005